X-RAY RADIOSCOPY OF LIQUID METALFOAMS: INFLUENCE OF HEATING PROFILE, ATMOSPHERE AND PRESSURE

Francisco García-Moreno[1,2], Norbert Babcsan[1,2], John Banhart[1,2]
[1] *Hahn-Meitner-Institute Berlin, Germany*
[2] *Technical University Berlin, Germany*

ABSTRACT

Metal foams are investigated in-situ and in real-time with help of X-ray radioscopy. The equipment consists mainly of 3 parts: 1) a microfocus X-ray source 2) a panel detector and 3) a small foaming heater, almost transparent for X-rays. For these work a novel x-ray transparent pressure heating systems for foaming under controlled atmosphere was developed and constructed. The control of the foaming temperature profile was found to be a determining factor for expansion and stability of metal foams. Moreover, other parameters such as foaming gas, foaming atmospheric pressure were also tested. Different expansion and stability behaviour on metallic foams was achieved using different temperature profiles. Expansion and average cell size also could be controlled adjusting the atmospheric foaming pressure. By foaming under high pressures extremly low average pore diameters could be reached. Foam behaviour under cyclical pressure variation was elastic and reversible in a certain range.

Keywords: metal foams, radioscopy, temperature profile, gas, pressure.

INTRODUCTION

In the past years metal foams have created a lot of scientific and industrial interest [1,2]. A range of ex-situ characterization methods have been applied to find optimal manufacturing parameters. In-situ X-ray radioscopy experiments show the evolution of metal foam morphology during the foaming process [3]. In the case of the powder metallurgical (PM) manufacturing route many precursor-related parameters such as the type and amount of blowing agent, its particle size and pre-treatment. [4] as well as alloy composition, mixture and compaction parameters, etc. can be varied. The influence on foaming behaviour and structure can be observed directly. Process parameters related to the foaming step such as foaming temperature, heating rate, etc. were also investigated [5]. The influence of the foaming gas atmosphere and hydrogen losses during the heating phase were assumed to be responsible for differences in expansion and stability. To prove these effects a novel X-ray pressure furnace was developed. The aim of this work is to investigate the effect of the temperature profile during foaming, the surrounding atmosphere and gas pressure on foaming kinetics of different precursors.

EXPERIMENTAL SETUP

A150 kV microfocus X-ray source with 5 μm spot size and a 2240 × 2368 pixels panel detector were used for radioscopy. Due to the cone beam geometry resolutions down to 5 μm at a magnification of 10 are possible. The maximal picture acquisition rate varies from 2 to 9 Hz depending on the time and spatial resolution requested.

With this equipment not only qualitative in-situ evaluation but also quantitative analysis of the recorded images can be performed using a self-developed software [3,5]. Time dependent values such as expansion, drainage rate, pore size distributions, cell wall rupture frequencies, etc. are calculated from the image series. As the samples were freely foamed without a mould and were not cylindrically shaped the expansion in beam direction cannot be calculated. Therefore we consider the relative cross section variation F/F_0 which is slightly smaller than the volume variation V/V_0 as a measure for expansion.

To allow radioscopic in-situ investigations of the influence of atmospheric gas composition and pressure on foaming behaviour, a novel X-ray transparent pressure heater was built. It consists of an Al-tube (∅ = 40 mm, l = 200 mm) with a wall thickness of d = 0.5 mm. The tube can be hermetically sealed at both ends with gas in- and outlets and electrical connectors. Inside the tube a resistive heating plate (500 W) is installed providing heating rates up to 35 K/s and a maximum temperature of 800 °C. The heater was designed and tested for a pressure range of 0.01 to 10 bar.

The foamable precursor material used was obtained by the PM hot pressing method. Thereby, Al99.7 and AlSi6Cu4 powders were mixed with a small amount (~ 0.5 wt%) of blowing agent (TiH_2) and uniaxially hot pressed in a die of ∅ = 36 mm at 300 kN and 400 °C for 5 minutes. Similar samples of around 5×10×20 mm^3 were prepared and freely foamed under different conditions.

RESULTS

Foaming conditions play a very important role for foam development and have a large influence on final pore structure. Several processes such as losses of hydrogen during heating, formation of oxide skins on the foam surface, gas pressure balance between pores and ambient atmosphere, cell wall stabilisation mechanisms, etc. are responsible for foam quality, but mostly overlapped and difficult to analyse. In order to investigate these effects separately different specially defined conditions during foaming were chosen, e.g. driving defined temperature profiles and foaming under different gas pressures and atmospheres.

Heating profile

Due to the small heat capacity of our heater we can heat up the system together with the sample in very short times. This way profiles with several steps and linear ramps up to 35 K/min are possible. Fig. 1a shows different heating profiles with 3 main steps: A starting high temperature ramp in step 1, different temperature evolutions in step 2 and the isothermal end temperature in step 3. Fig. 1b shows the corresponding foam expansion

kinetic to fig. 1a.

Gas composition

Different gas atmospheres (oxygen, argon) could influence stability of foams, e.g. due to the formation of oxide skins under oxygen influence. This effect was seen before for AlSiMg-alloys [6]. For AlSi6Cu4 foamed under air and argon at 1 bar no great difference in expansion and stability could be measured. For samples foamed under 8 bar followed by a pressure reduction to 1 bar with – 0.2 bar/s a reduced expansion could be found for argon compared to air (Fig. 2). In addition, big bubbles at the foam surface as well as a more shiny surface skin could be observed in the case of argon.

Gas pressure

Radioscopic pictures of foaming under a reduced pressure of 0.01 and 0.1 bar air were performed (Fig. 3) and compared with a standard pressure of 1 bar. For AlSi6Cu4 with 0.5 wt% TiH_2 it was found that under these conditions no stable foam can be produced. Cell wall stability is not given. In a first stage the precursor begins to expand and forms the cracks characteristic for the PM route by uniaxial hot pressing. Directly after metal melting gas escapes from the surface of the precursor material and the sample appears like boiling water . After a certain time coarsening leads to very big bubbles (Fig. 3) that start to grow and rise after a few seconds. Drainage increases more and more and at the end we cannot speak of a metal foam anymore but only of molten metal.

More interesting foaming results were obtained under overpressure. In this case Al99.7 precursors with 0.5 wt% TiH_2 were foamed in air at 1, 3, 5 and 8 bar (Fig. 4a). Beside an expansion reduced by a factor of $F_1/F_2 \sim 2$ at 8 bar, a notably increasing homogeneity of the pore size distribution and a reduction of the average pore size could be found with increasing pressure. Just by changing the pressure in the furnace expansion can be controlled, but also the technologically more important average pore size d_p, in this case by a factor of 10, from $d_p \sim 0.1$ mm at 8 bar to $d_p \sim 1$mm at 1 bar. In a second step (Fig. 4b) the overpressures were released to 1 bar after a holding time of 30 s. Surprisingly, the resulting final foam expansion increases with the pressure first applied, while pore homogeneity decreases. For AlSi6Cu4 the effect is even more pronounced: expansion could be reduced from $F/F_0 \sim 4$ at 1 bar to $F/F_0 \sim 1.5$ at 8 bar after several cycles (Fig. 5).

To investigate the influence of the variation of ambient pressure on liquid metal foams completely expanded and stable samples were subjected to several pressure cycles (Fig. 5 and 6). A largely reversible plastic behaviour of the liquid foam was found. Foam volume oscillated between a minimum and a maximum value with a continuous increase of the maximum. Comparison of two radioscopic pictures before and after one cycle shows clearly that even pore size structure persists when reaching the original expansion without coalescence up to this point. During the additional expansion high coalescence can be observed until the next high pressure cycles begin. After 5 or 6 cycles this effect saturates out and neither increased expansion nor additional coalescence can be found.

DISCUSSION

Heating profile

By the standard PM foaming route the precursor material is introduced into a pre-heated furnace at a fixed temperature. Depending on the mass of the sample, the heating power of the furnace and the thermal capacity of the mould (if used at all) the precursor material reaches the foaming temperature more or less quickly following an asymptotic profile. Such an asymptotic behaviour is considered non-optimal since ideally the heating rate should be as high as possible up to the beginning of the desorption temperature of TiH_2 (~400 °C) to avoid hydrogen losses and gas agglomerations as much as possible during this heating phase, when the metal is still solid. For the first step in Fig. 1 we used a relatively high heating rate of ~200 K/min. In a previous study [5] it was shown that for this alloy the critical heating rate of 50 K/min should be exceeded. The second step begins just after reaching the foaming temperature when expansion begins. Sample 1 shows the foaming behaviour typical for overheating (max. 750 °C) characterised by high and rapid expansion with a sharp maximum followed by fast collapse and strong coalescence. The reason for this seems to be the missing cell wall stabilisation in this phase. Sample 2 is as well overheated up to 700 °C, reaching an end temperature of 650 °C in the third step. The maximum expansion is similar to that of sample 1, but decay and collapse are more moderate. Sample 3 and 4 are more stable in step 2 and 3. Here a slower heating in step 2 provides stable foams with different end expansions depending on the end temperatures. In these two latter cases the foams are about 100 s longer below or around the liquidus temperature T_L ~ 615 °C, maintaining stability also after further temperature increase. It seems that in the early expansion the stabilisation process is given by the still solid particles, the so-called endogenous stabilisation [7], before other stabilisation mechanisms such as oxide fragments [8], which act as effective particles, etc. can provide a stable foam even at 700 °C for at least over 700 s. Anyhow, looking at the course of the three steps of sample 2 it becomes obvious that a fast heating ramp up to 550°C followed by the traditional asymptotic heating profile is a good approach to the best result. It becomes clear that any overheating during foaming is deleterious and should be avoided.

Gas composition

For AlSi6Cu4 no significant influence of the gas atmosphere was found. Possibly, surface oxide skins do not to play an important role in these alloys as no significant expansion differences were found under air and argon. However, the reason may also be that the formation of oxide skins even under argon cannot be avoided due to residual oxygen traces in the gas or to oxides or hydroxides already contained in the compacted powders. At least in the case of foaming under 8 bar with subsequent pressure release to 1 bar a reduced expansion under argon in the second step was found. That stability is reduced only after the second expansion step, may be explained by an insufficient coverage of the film surface with oxides. This would also explain the big surface bubbles and the shiny appearance in the sample foamed under argon. Further experiments with oxygen reduction and more

reactive alloys containing e.g. Mg have to be carried out.

Gas pressure

Under reduced ambient pressure hydrogen losses during heating may be higher than under normal pressure due to the increased internal pressure relative to the ambient atmosphere, although this effect seems not to be very important because the initial expansion phase is very similar to the one under normal pressure. However, in a later stage after first bubble formation the internal gas pressure is relatively high. No foam stabilization mechanisms can keep the balance between buoyancy and metal weight, so that bubbles rise to the surface and instability and strong coalescence are observed. On the other hand it is necessary to remember that the manufacturing parameters were optimised for foaming under 1 bar, that means with e.g. a reduction of blowing agent contents down 0.5 wt% better results could be obtained. This will be investigated in future.

A reduced expansion under overpressure can be easily explained due to the force balance between bubbles and ambient pressure. The extremely reduced average pore diameter indeed not. Fig. 4 left shows clearly that if we will reduce the image of the foam foamed under 1 bar to the size of e.g. the foam under 8 bar the average pore size will be greater. That means the number of nucleated pores under 8 bar is much higher than under 1 bar and that the overpressure the nucleation number influences. An explanation for this could be, that the hydrogen release under overpressure is less or shifted to a later moment. Another effect to consider is the pressure p dependence of the amount of hydrogen c_H dissolved in the molten Al, that following Sieverts law corresponds to $c_H \sim \sqrt{p}$, that means under high pressure more hydrogen will be dissolved and less will be available for the pore formation. In our experiment this means for $\Delta p = 7\ bar$ the dissolved hydrogen factor by 8 bar is c_H = 2.65 more than by 1 bar. In these two cases pores will lead to less gas agglomeration during the early foaming stages and therefore to an increased gas nucleation and pore number. After pressure release to 1 bar expansion is even higher as by direct foaming under 1 bar. The reason for this could be, that during foaming less hydrogen is lost due to the overpressure of the surrounding. After the second pressure step the expansion is consequently higher due to the increased gas resources. Another possibility could be, that the bubble pressure in the pores increases due to gas diffusion into the foam. An evidence for this can be found on fig. 2, where the expansion of an under 8 bar stable foam $F/F_0 \sim$ 2.25 before and $F/F_0 \sim$ 2.75 after a 120 s 1 bar cycle was.

It could be shown that the maximal expansion increases after several pressure cycles. Furthermore the pore structure is maintained until the previous maximum expansion is reached, showing an exceptionally reversible behaviour, without coalescence. In the high pressure phases pores are not spherical, but flat. During the additional expansion high coalescence can be found. All these phenomena indicate the existence of a more or less rigid, stabilising but flexible cell wall skin that cannot shrink, but fracture by pressure induced additional expansion.

SUMMARY

X-ray radioscopy was used for in-situ real-time experiments on metallic foams. An optimised temperature profile based on 3 steps was found to provide the best expansion and stability results. Foaming under argon shows surface bubbles and a shiny skin only under 8 bar with subsequent pressure release to 1 bar. A great influence of the gas pressure on the foaming behaviour was found. Under low pressures high coalescence, instabilities and rising big bubbles characterise the foams. Under high pressures, beside a reduced expansion, an extremely small average cell size and high homogeneity was observed. Release from high pressure to normal pressure leaded in an increased expansion. Also reversible expansion and compression after several pressure cycles were found, with a flexible cell wall structure. An additionally expansion with high coalescence followed each cycle, increasing the maximal expansion from $F/F_0 \sim 1.5$ at 8 bar to $F/F_0 \sim 4$ at 1 bar.

Acknowlegements: Funding by ESA (Project AO-99-075) and DFG (Ba 1170/3-3) is gratefully acknowledged. We also thank Dr. Uwe Laun for his help building the pressure furnace.

REFERENCES

[1] F. Baumgärtner, I. Duarte, J. Banhart, Adv. Eng. Mater. 2, 168-174 (2000)
[2] H.-W. Seeliger, Proc. Int. Conf. Metal Foams and Porous Metal Structures, Eds. J. Banhart, M.F. Ashby, N.A. Fleck, (MIT-Verlag Bremen), 29-36 (1999)
[3] García Moreno, F., Fromme, M., Banhart J., in "Cellular Metals", eds. J. Banhart, N.A. Fleck, A. Mortensen, MIT-Verlag Berlin (2003), p. 89
[4] B. Matijasevic, S. Fiechter, O. Görke, I. Zizak, N. Wanderka, P. Schubert-Bischoff, J. Banhart, Proc. Int. Conf. Powder Metallurgy 2004, Vienna, October 17-21, to be published
[5] F. Garcia-Moreno, M. Fromme, and J. Banhart, Adv. Eng. Mater. 6, 416-420 (2004)
[6] F. Simancik, K. Behulova, and L. Bors, Proc. Int. Conf. Cellular Metals and Metal Foaming Technology, Eds. J. Banhart, M.F. Ashby, N.A. Fleck, (MIT-Verlag Bremen), p. 89-92 (2001)
[7] C. Körner, M. Hirschmann, V. Bräutigam, and R. F. Singer, Adv. Eng. Mater. 6, 385-390 (2004)
[8] M. Arnold, C. Körner, R. F. Singer, in "Cellular Metals", eds. J. Banhart, N.A. Fleck, A. Mortensen, MIT-Verlag Berlin (2003), p. 209

Captions

Figure 1: a) Different temperature profiles with three main steps. b) Foam expansion kinetics corresponding to samples in a)

Figure 2: Foam expansion kinetics under different gases and pressures. Radioscopic images at max. expansion. Arrow: surface bubbles.

Figure 3: AlSi6Cu4 foamed under low pressures. Radioscopic images at max. expansion.

Figure 4: Radioscopic images of Al99.7 samples a) foamed at different pressures and b) after pressure release to 1 bar.

Figure 5: Expansion kinetics corresponding to the sample in fig. 6

Figure 6: Radioscopic images of AlSi6Cu4 after several pressure cycles, a) under 1 bar and b) under 8 bar.

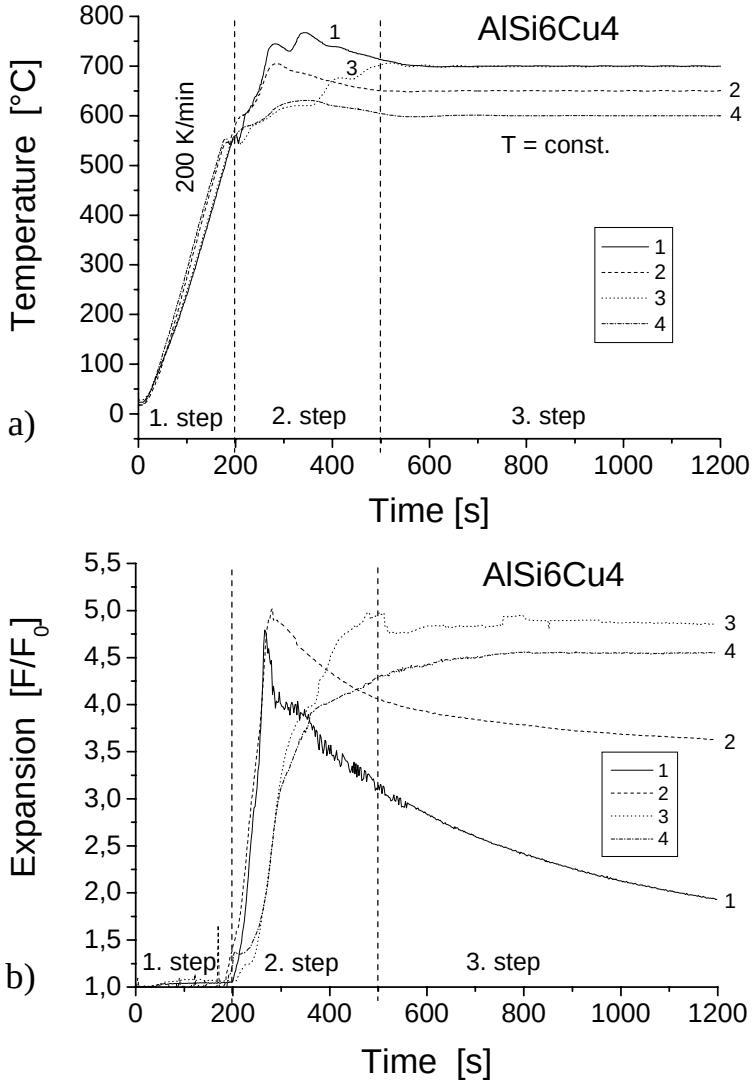
AlSi6Cu4
Temperature [°C]
200 K/min
T = const.
1
2
3
4
1. step
2. step
3. step
Time [s]
a)
AlSi6Cu4
Expansion [F/F0]
1. step
2. step
3. step
Time [s]
b)

Fig. 1

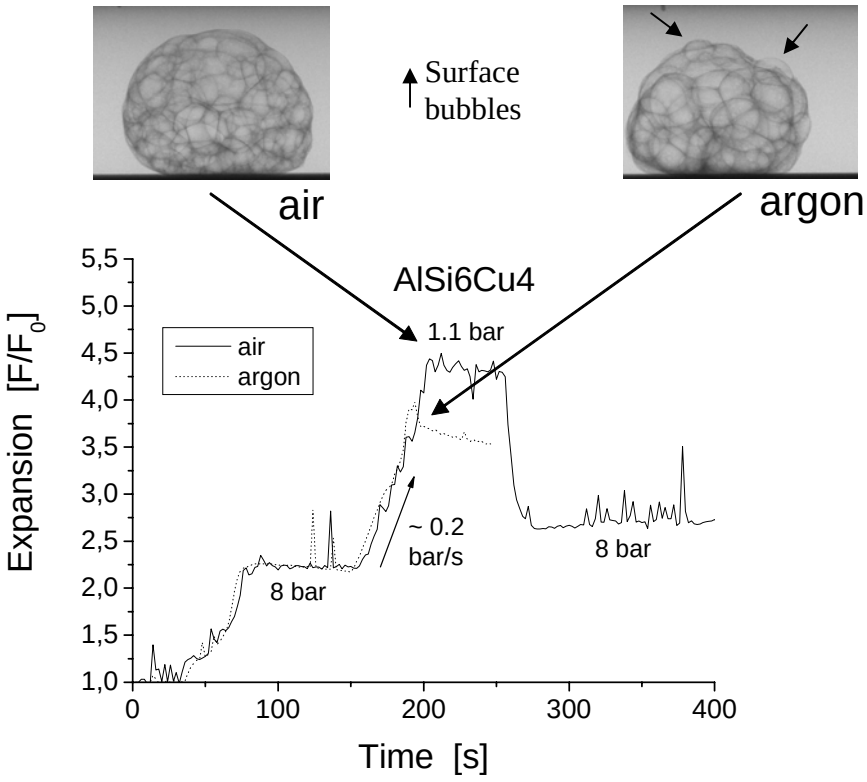
Surface
bubbles
air
argon
AlSi6Cu4
1.1 bar
air
argon
~ 0.2
bar/s
8 bar
8 bar
Expansion [F/F0]
Time [s]
5,5
5,0
4,5
4,0
3,5
3,0
2,5
2,0
1,5
1,0
0
100
200
300
400

Fig. 2

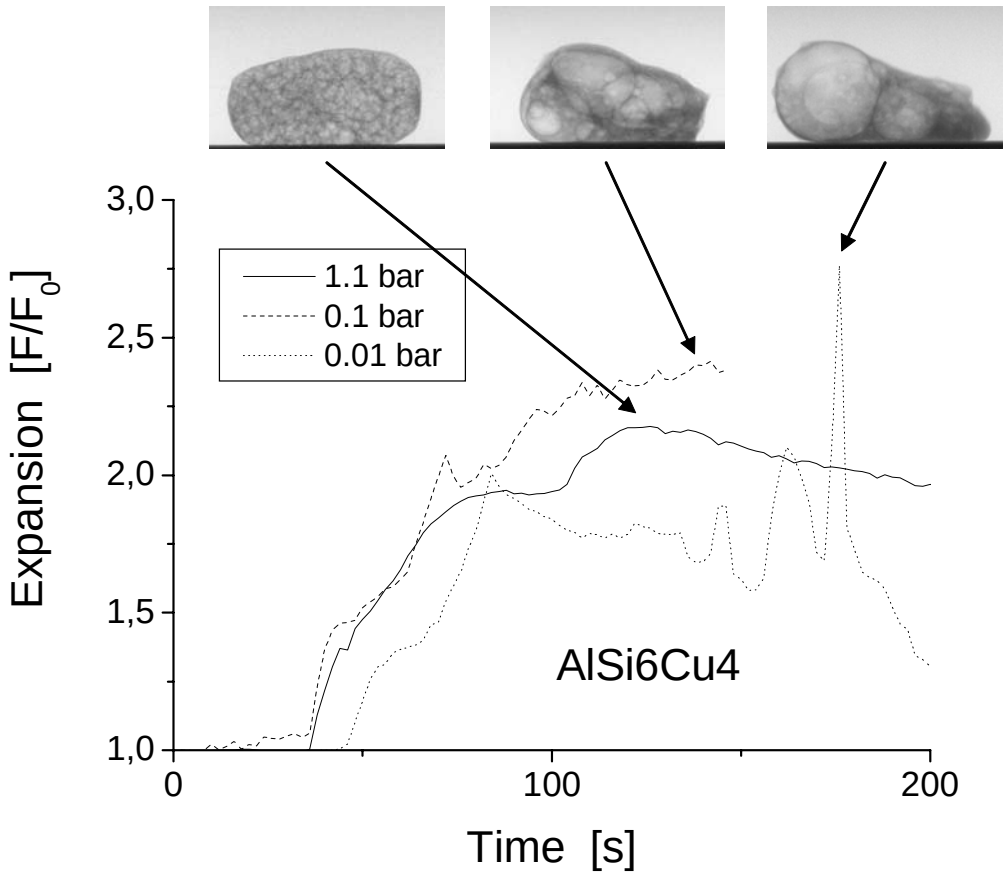
3,0
2,5
2,0
1,5
1,0
Expansion [F/F0]
1.1 bar
0.1 bar
0.01 bar
AlSi6Cu4
0
100
200
Time [s]

Fig. 3

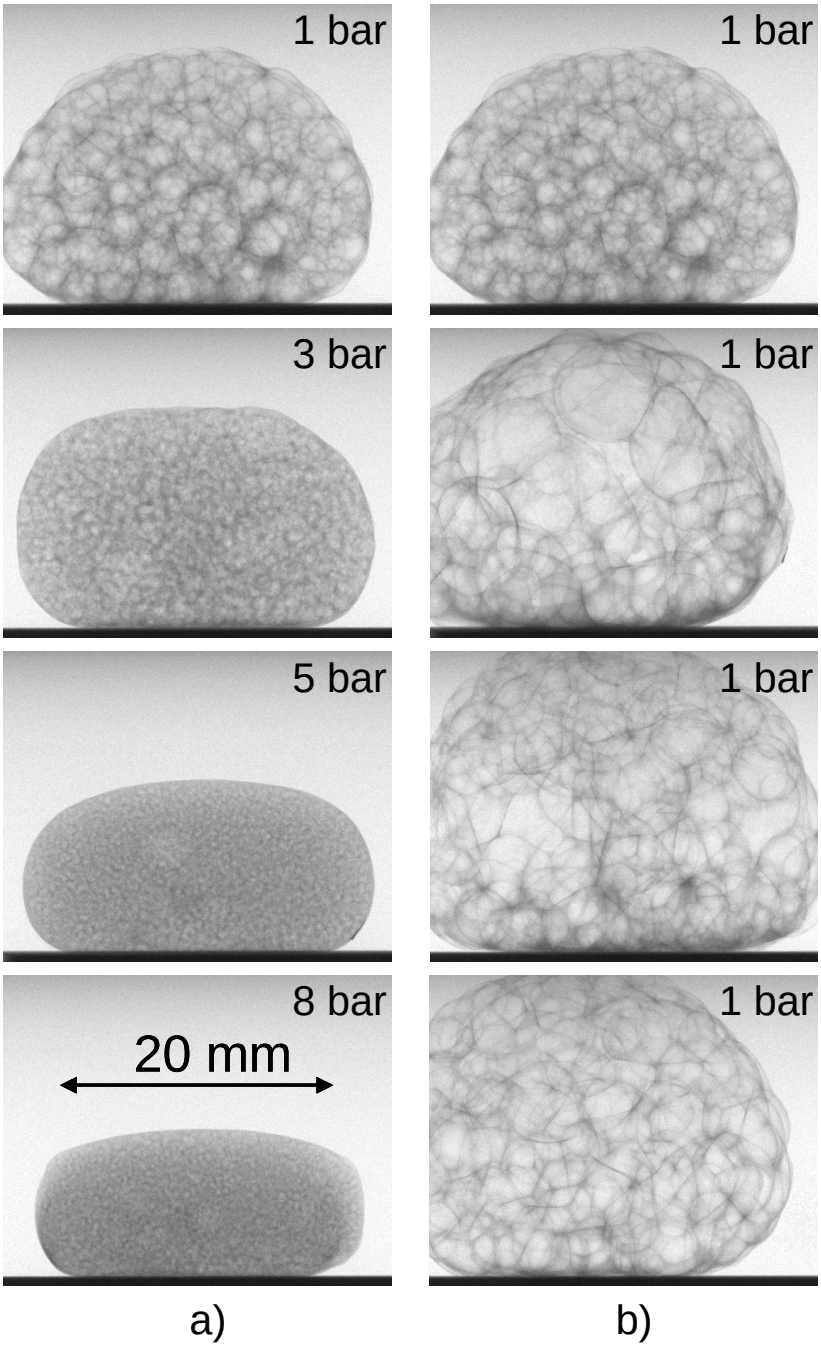

Fig. 4

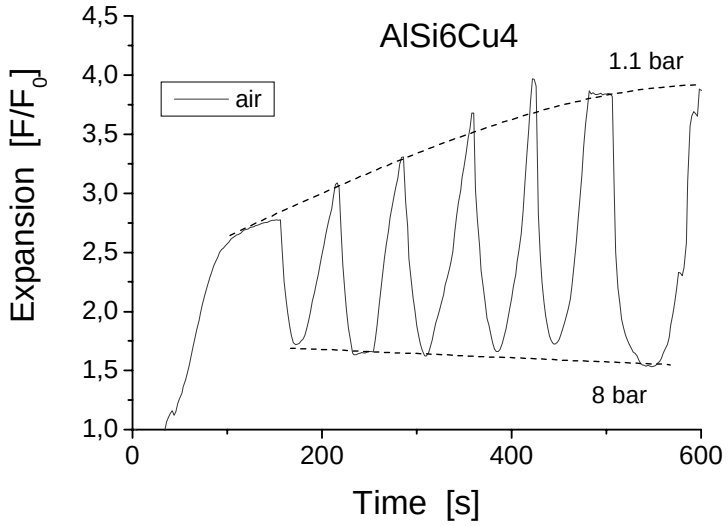
AlSi6Cu4
1.1 bar
air
8 bar
Expansion [F/F0]
Time [s]
4,5
4,0
3,5
3,0
2,5
2,0
1,5
1,0
0
200
400
600

Fig. 5

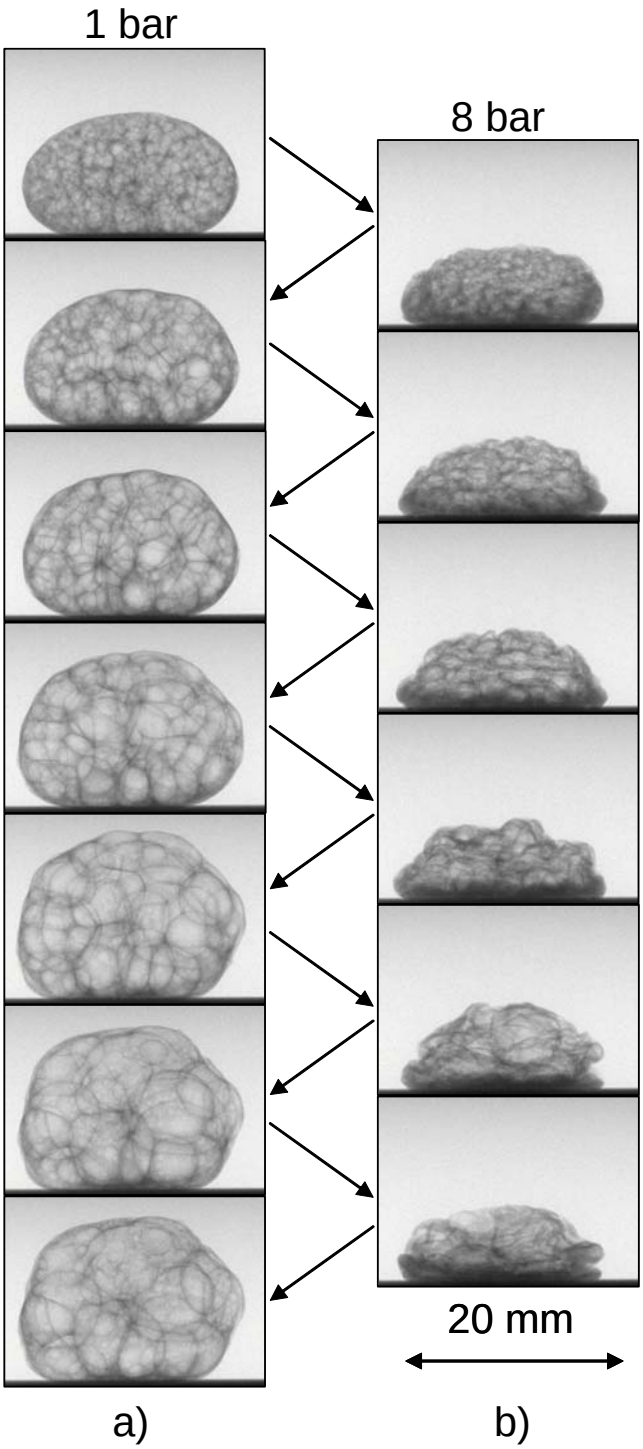

Fig. 6